

Synthesis, Structures, and Optical Properties of Two Novel Two-Photon Initiators Derived from 2,2′:6′,2″-Terpyridine

Zhang-Jun Hu,[1] Jia-Xiang Yang,*[1,2] Yu-Peng Tian,*[1,2] Xu-Tang Tao,[2] Lei Tian,[1] Hong-Ping Zhou,[1] Gui-Bao Xu,[1] Wen-Tao Yu,[1] Yun-Xing Yan,[2] Yuan-Hong Sun,[3] Chuan-Kui Wang,[3] Xiao-Qiang Yu,[2] and Min-Hua Jiang[2]

[1]Department of Chemistry, Anhui University, Hefei 230039, P. R. China

[2]State Key Laboratory of Crystal Materials, Shandong University, Jinan 250100, P. R. China

[3]Department of Physics, Shandong Normal University, Jinan 250014, P. R. China

Received August 22, 2006; E-mail: jxyang@ahu.edu.cn

Efficient aqueous-phase aldol condensation, Michael addition, and solvent-free Wittig reactions were successfully employed to synthesize two two-photon initiators 9-ethyl-3-[4-(2,2′:6′,2″-terpyridinyl-4′-yl)styryl]carbazole (**T1**) and 9-{4-[4-(2,2′:6′,2″-terpyridinyl-4′-yl)styryl]phenyl}carbazole (**T2**). The two initiators with carbazolyl moiety attached to 2,2′:6′,2″-terpyridine present D–π–A-type framework, where A is a π-deficient terpyridine ring. The crystal structures were determined by single-crystal X-ray diffraction determination. The experimental results confirmed that the two initiators have sensitive single-photon-excited fluorescence (SPEF) and two-photon-excited fluorescence (TPEF) properties. The experimental and theoretical two-photon absorption (TPA) cross-sections were investigated. Two-photon initiation polymerization (TPIP) microfabrication experiments were carried out, and possible polymerization mechanisms are discussed based on the theoretical evaluation.

Materials with a large TPA cross-section have attracted considerable attention due to their various applications in the areas of optical limiting,[1] two-photon photodynamic therapy,[2] two-photon-pumped up-conversion lasing,[3] three-dimensional (3D) fluorescence imaging,[4] optical data storage,[5] and the two-photon micro-fabrication (TPMF).[6,7] As far as the TPMF technique is concerned, it has paved a way to direct laser fabrication of 3D microstructures in one step with high spatial resolution, making possible many applications, such as photonic devices, micromachines, zero-threshold lasers, and integrated optical waveguides.[8,9]

TPIP is the most important approach to realize TPMF, which utilizes high-efficient two-photon initiators and excites them by laser pulses in the near IR region. However, efficient two-photon initiators are still not abundant. Therefore, a control of the molecular geometry as well as the electronic structure and optimization of the physical properties of the initiators to develop the new initiators is of crucial importance to prepare more efficient TPIP initiators. Recently, many D–π–D-type initiators have been developed.[6] Our group also have developed a series of two-photon initiators with symmetric and asymmetric molecular structure of types: A–π–D–π–A, D–π–A, and D–π–D. These initiators show efficient TPA and were applied in TPIP successfully.[6c,7] Although these TPA dyes, based on conjugated aromatic rings, are now available, some complicated hetero-aromatic compounds, which are often used for special purposes in the two-photon area due to their favorable coordinate abilities, such as 2,2′:6′,2″-terpyridine with a rigid framework plane and a superb ability to coordinate with various metal ions, are still not well explored.[10] Its derivatives are often used for many physical and chemical applications.[11] Recently, there have been a few reports about TPA response of some D–π–A-type terpyridine derivatives.[12] The recent success of the research on green and facile preparations of the key precursor 1,5-di(2-pyridinyl)-3-*p*-tolylpentane-1,5-dione (**3′**)[13] has aroused our interests in studying these derivatives from a two-photon-initiator point of view. By incorporating carbazolyl unit into the terpyridine backbone, D–π–A-type initiators, in which the terpyridyl ring is the acceptor part and a carbazolyl group the donor one, were prepared.

In this work, a facile synthesis route for precursor compound 2,2′:6′,2″-terpyridine involving aqueous-phase aldol condensation and Michael addition reactions, is presented. Furthermore, solvent-free Wittig reactions were used in building the π-conjugated system. The single-crystal structures and the linear/nonlinear optical properties of two compounds as well as a brief discussion about the relationships of structure/properties are described. TPIP microfabrication experiments demonstrated that they could act as efficient two-photon photopolymerization initiators. A possible mechanism of the photopolymerization is discussed.

Experimental

Instruments and Measurements. The ^{1}H NMR and ^{13}C NMR spectra were recorded at 25 °C on a Bruker Avance 500 or 600 spectrometer, and the chemical shift are reported as parts per million (ppm) from TMS (δ). Coupling constants J are given in Hertz. Mass spectra were acquired on a Micromass GCT-MS (EI source). Elemental analysis was performed on a Perkin-Elmer 240 instrument. The melting points were measured on a METTLER-

Published on the web May 14, 2007; doi:10.1246/bcsj.80.986

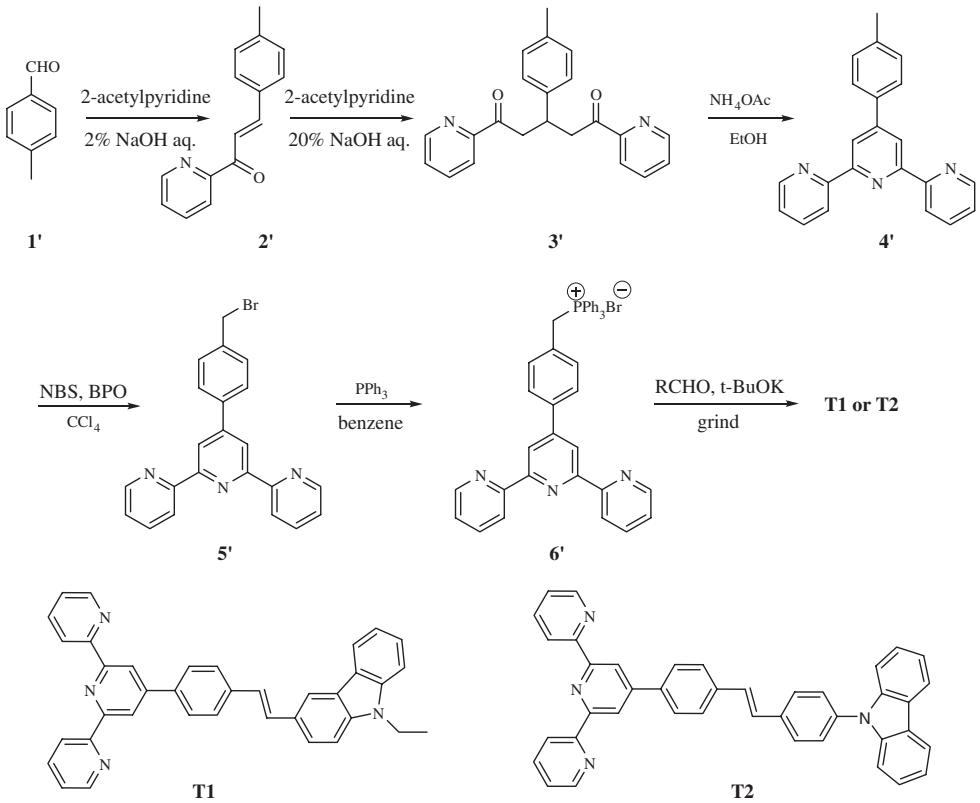

Scheme 1. Synthesis strategy for the preparation of two initiators (RCHO = 9-ethylcarbazole-3-carbaldehyde (**a**) and 4-(9-carbazolyl)benzaldehyde (**b**)).

TOLEDO DSC822 differential scanning calorimeter at a heating rate of 20 °C min^{-1} under a nitrogen atmosphere. IR spectra were recorded on a NEXUS 870 (Nicolet) spectrophotometer in the 400–4000 cm^{-1} region using a powder sample on a KBr plate.

X-ray diffraction data of single crystals were collected on a Siemens Smart 1000 CCD diffractometer and a Bruker P4 four-circle diffractometer. The determination of unit cell parameters and data collections were performed with Mo Kα radiation (λ = 0.71073 Å). Unit cell dimensions were obtained with least-squares refinements, and all structures were solved by direct methods using SHELXS-97. The other non-hydrogen atoms were located in successive difference Fourier syntheses. The final refinement was performed by using full-matrix least-squares methods with anisotropic thermal parameters for non-hydrogen atoms on F^2. The hydrogen atoms were added theoretically and riding on the concerned atoms.

UV–vis absorption spectra were recorded on a UV-3100 spectrophotometer. Fluorescence measurements were carried out using an Edinburgh FLS920 fluorescence spectrometer equipped with a 450 W Xe lamp and a time-correlated single-photon counting (TCSPC) card. All the fluorescence spectra were collected. The SPEF quantum yields Φ were measured by using a standard method under the same experimental conditions for all compounds. Coumarin 307 dissolved in ethanol ($\Phi = 0.56$)[14] at the same concentration as the other sample was used as the standard. Lifetime values were obtained by reconvolution fit analysis of the decay profiles with the aid of F900 analysis software. The fitting results were judged by their values of "reduced chi-squared." TPEF spectra and TPIP microfabrication were measured using a mira 900-D Ti:sapphire femtosecond laser with a pulsewidth of 200 fs and a repetition rate of 76 MHz. All measurements were carried out in air at room temperature. TPA cross-sections were measured using flouorescein as reference.

Materials and Synthesis. All chemicals were available commercially, and the solvents were purified as conventional methods before use. 9-Ethylcarbazole-3-carbaldehyde (**a**), 4-(9-carbazolyl)-benzaldehyde (**b**) were synthesized according to the reported methods.[15] As shown in Scheme 1, we synthesized the title compounds by a series of modified reactions. The *trans*-isomer products were recrystallized from different solvents. These compounds were characterized by ^{1}H NMR, ^{13}C NMR, FT-IR, and MS spectrometry.

4′-(*p*-Tolyl)-2,2′:6′,2″-terpyridine (4′): A flask charged with 2-acetylpyridine (3.0 g, 24.8 mmol), freshly distilled 4-methylbenzaldehyde (**1′**) (3.0 g, 24.8 mmol) and 2% aqueous sodium hydroxide (100 mL) was vigorously stirred for about 8 h at room temperature, during which time a bright yellow solid product **2′**, that was not isolated precipitated. Another molar amount of 2-acetylpyridine (3.0 g, 25.0 mmol) was added into the preceding reaction system and the concentration of aqueous sodium hydroxide was changed from 2 to 20%. The reaction was monitored by TLC. After another 8 h of constant stirring at 80 °C, a dark-brown ropy mixture containing 1,5-di(2-pyridyl)-3-*p*-tolylpentane-1,5-dione (**3′**) were gained after removing the aqueous phase. The ropy mixture was added to a stirred solution of ammonium acetate (18.0 g, excess) in ethanol (250 mL). The reaction was heated at reflux for 5 h, affording a dark red solution. Cooled to the room temperature, bright yellow product was crystallized from the filtered solution. The white acicular product was recrystallized from ethanol and dried in vacuum to give **4′** (6.0 g, 75%). Mp: 167.8 °C. ^{1}H NMR ($CDCl_3$, 600 MHz): δ 2.44 (s, 3H), 7.33 (d, J = 7.87 Hz, 2H), 7.39 (t, J = 6.05 Hz, 2H), 7.85 (d, J = 7.87 Hz, 2H), 7.92 (t,

$J = 7.38$ Hz, 2H), 8.70 (d, $J = 7.87$ Hz, 2H), 8.76 (m, 4H). ^{13}C NMR ($CDCl_3$, 600 MHz): δ 156.27, 155.77, 150.18, 149.04, 139.09, 136.91, 135.41, 129.63, 127.14, 123.77, 121.38, 118.65, and 21.23. MS: m/z (%) = 324.15 (100). FT-IR (KBr, cm^{-1}): $\nu = 3774$, 3702, 3049, 1581, 1468, 1391, 1262, 1036, 882, 821, 790, 728, 687, 615, 492.

4′-[4-(Bromomethyl)phenyl]-2,2′:6′,2″-terpyridine (5′): Compound **4′** (5.0 g, 15.5 mmol), NBS (2.9 g, 16.1 mmol) and a catalytic amount of benzoyl peroxide (BPO) were dissolved in anhydrous tetrachloromethane (200 mL). The mixture was refluxed for 8 h. After the mixture cooled to room temperature, the solid residue was filtered. The filtrate was washed with water and brine and then dried over anhydrous magnesium sulfate. After filtration and solvent evaporation, the residual solid was recrystallized from anhydrous ethanol, to give 5.0 g white crystals **5′** in an 80% yield. Mp: 176 °C. ^{1}H NMR ($CDCl_3$, 600 MHz): δ 4.58 (s, 2H), 7.38 (m, 2H), 7.56 (d, $J = 8.00$ Hz, 2H), 7.90 (m, 4H), 8.69 (d, $J = 8.00$ Hz, 2H), 8.45–8.77 (m, 4H). ^{13}C NMR ($CDCl_3$, 400 MHz): δ 156.07, 155.95, 149.50, 149.09, 138.62, 138.57, 136.94, 129.63, 127.76, 123.89, 121.38, 118.82, and 32.96. MS: m/z (%) = 324.15 (100), 404.05, 401.05, 405.06. FT-IR (KBr, cm^{-1}): $\nu = 3779$, 3697, 3635, 3049, 1807, 1719, 1658, 1581, 1483, 1386, 1221, 1031, 893, 831, 785, 738, 672, 590, 492.

4-(2,2′:6′,2″-Terpyridin-4′-yl)-benzyltriphenylphosphonium Bromide (6′): A mixture of **5′** (5.0 g, 12.4 mmol) and triphenylphosphine (TPP) (4.9 g, 18.6 mmol) in anhydrous benzene (150 mL) was refluxed for 18 h. The product was precipitated from the resulting solution. The off-white precipitates were collected via filtration and dried under vacuum to give **6′** (7.4 g, yield 90%). It was used in the next reactions without characterization.

9-Ethyl-3-[4-(2,2′:6′,2″-terpyridinyl-4′-yl)styryl]carbazole (T1): *t*-BuOK (1.3 g, 12.3 mmol) was placed into a dry mortar and milled to very small, then **6′** (2.0 g, 3.0 mmol) and **a** (0.7 g, 3.14 mmol) were added and mixed. The mixture was milled vigorously for about 20 min. The mixture became sticky, and then tetrahydrofuran (5 mL) was added. The mixture was continuously milled for another 10 min. After completion of the reaction (monitored by TLC), the mixture was dispersed in 100 mL ethanol. The residual solid was filtered and recrystallized from anhydrous dichloromethane/ethanol, to give yellow crystals **T1** (1.3 g, yield 80%). Mp: 310 °C. ^{1}H NMR ($CDCl_3$, 500 MHz): δ 1.49 (t, $J = 7.23$ Hz, 3H), 4.42 (q, $J = 7.23$ Hz, 2H), 7.24 (d, $J = 16.3$ Hz, 2H), 7.25–7.30 (m, 2H), 7.40–7.53, (m, 6H), 7.73 (t, $J = 6.75$ Hz, 3H), 7.95 (t, $J = 7.57$ Hz, 2H), 8.00 (d, $J = 8.13$ Hz, 2H), 8.17 (d, $J = 7.67$ Hz, 1H), 8.30 (s, 1H), 8.74 (d, $J = 7.92$ Hz, 2H), 8.80 (d, $J = 4.45$ Hz, 2H), 8.85 (s, 2H). ^{13}C NMR ($CDCl_3$, 600 MHz): δ 157.57, 156.17, 155.76, 148.95, 140.43, 139.92, 138.97, 137.13, 130.65, 128.43, 127.61, 126.74, 125.88, 125.29, 124.59, 123.87, 123.40, 123.03, 121.53, 120.54, 119.12, 118.98, 118.68, 108.71, 108.66, 98.13, 25.37, and 13.86. MS: m/z (%) = 528.23 (100), 513.19 (84). FT-IR (KBr, cm^{-1}): $\nu = 3047$, 2972, 1584, 1564, 1468, 1441, 1387, 1344, 1328, 1230, 1151, 1126, 1081, 1037, 962, 821, 792, 738, 685, 661, 623, 514. Calcd for $C_{37}H_{28}N_4$ (528.7): C, 84.06; H, 5.34; N, 10.60%. Found: C, 84.13; H, 5.20; N, 10.12%.

9-{4-[4-(2,2′:6′,2″-Terpyridinyl-4′-yl)styryl]phenyl}carbazole (T2): Compound **T2** was also prepared similarly to **T1** via **b** and **6′** to afford solid product (yield 83%). ^{1}H NMR (DMSO-d_6, 600 MHz): δ 7.30–7.70 (m, 12H), 7.8–8.30 (m, 10H), 8.60–8.80 (m, 6H). ^{13}C NMR ($CDCl_3$, 600 MHz): δ 156.40, 156.08, 149.91, 149.15, 141.09, 138.20, 137.95, 137.37, 137.19, 136.65, 128.78, 128.18, 127.90, 127.47, 127.36, 126.14, 124.00, 123.72, 121.67, 120.47, 120.20, 118.94, and 110.03. MS: m/z (%) = 578.23 (100), 288.12 (2.91). FT-IR (KBr, cm^{-1}): $\nu = 3415$, 3046, 1583, 1514, 1446, 1388, 1226, 1113, 1036, 968, 897, 833, 791, 745, 631, 582, 536. Calcd for $C_{41}H_{28}N_4$ (576.7): C, 85.39; H, 4.89; N, 9.72%. Found: C, 84.40; H, 4.78; N, 9.70%.

Crystallographic Data. Crystallographic data have been deposited with Cambridge Crystallographic Data Centre: Deposition number CCDC-228394 for **T1** and CCDC-228395 for **T2**. Copies of the data can be obtained free of charge via www: http://www.ccdc.cam.ac.uk/conts/retrieving.html (or from The Cambridge Crystallographic Data Centre, 12, Union Road, Cambridge, CB2 1EZ, UK; fax: +44 1223 336033; e-mail: deposite@ccdc.cam.ac.uk). Structural factors are available on request from the authors.

Results and Discussion

Structure Features. Single crystals of **T1**, suitable for the X-ray analysis, were obtained from slow evaporation of CH_2Cl_2 covered with 2-propanol at room temperature several days later. A structure is shown in Fig. 1. Crystal data are listed in Table 1. In the electron-acceptor moiety (terpyridinyl end), the center pyridinyl plane is labeled P0. The other three ring planes (labeled P2, P3, and P4) were arranged with dihe-

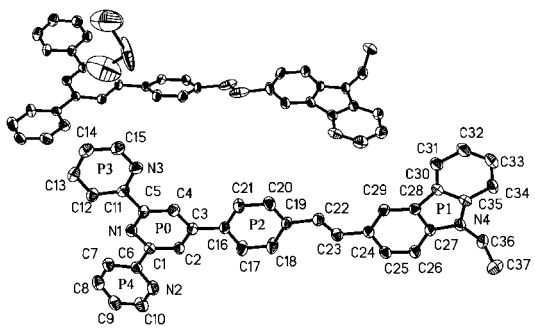

Fig. 1. Crystal structure of **T1**, arranged perpendicularity in a crystal. Hydrogen atoms are omitted for clarity.

Table 1. Crystal Data Collection and Structure Refinement of the Two Initiators

	T1	**T2**
Formula	$C_{75}H_{58}Cl_2N_8$	$C_{41}H_{28}N_4$
Formula weight	1142.17	576.67
Crystal system	Triclinic	Orthorhombic
Space group	$P\bar{1}$	*Pbcn*
Temperature/K	298(2)	293(2)
λ of Mo Kα/Å	0.71073	0.71073
Absorption coefficient/mm^{-1}	0.071	0.075
a/Å	11.853(5)	13.286(17)
b/Å	13.683(6)	22.946(3)
c/Å	19.596(9)	9.936(11)
α/°	108.393(8)	
β/°	94.379(8)	
γ/°	94.826(8)	
V/Å^3	2987.0(2)	3028.9(6)
Z	2	4
Reflections collected	15895	3445
Reflections unique	10400	2673
R_{int}	0.0570	0.0464
Final R indices[$I > 2\sigma(I)$]	$R_1 = 0.0725$, $wR_2 = 0.1683$	$R_1 = 0.0606$, $wR_2 = 0.1326$

Table 2. Selected Bond Lengths (Å) and Angles (°) of the Two Initiators

T1			
C(19)–C(22)	1.459(6)	C(22)–C(23)	1.301(6)
C(23)–C(24)	1.455(6)	N(4)–C(27)	1.377(5)
N(4)–C(35)	1.388(6)	N(4)–C(36)	1.462(6)
C(3)–C(16)	1.478(6)	C(5)–C(11)	1.469(7)
C(1)–C(6)	1.490(7)	C(27)–N(4)–C(36)	126.4(5)
C(27)–N(4)–C(35)	108.2(4)	C(35)–N(4)–C(36)	125.4(4)
T2			
C(10)–C(11)	1.493(5)	C(11)–C(12)	1.338(5)
C(13)–C(12)	1.484(5)	C(6)–N(1)	1.392(6)
C(7)–N(1)	1.429(7)	C(19)–C(20)	1.480(6)
C(16)–C(17)	1.487(8)	C(6)#1–N(1)–C(7)	125.9(3)
C(6)–N(1)–C(6)#1	108.2(6)	C(6)–N(1)–C(7)	125.9(3)

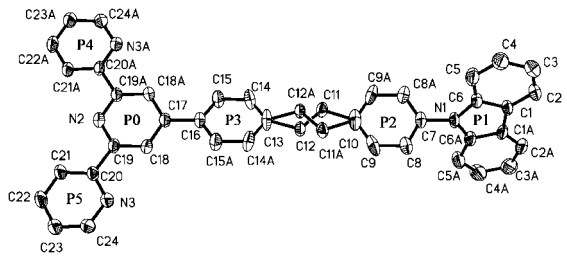

Fig. 2. Crystal structure of **T2**. Hydrogen atoms are omitted for clarity.

dral angles of 9.6° between P0 and P2, 11.6° between P0 and P3 and 10.6° between P0 and P4. At the *N*-based donor end, carbazolyl was basically co-planar (labeled P1), which may cause the delocalization of the lone pair of electrons into the π-system. The dihedral angle between P1 and the phenyl plane P2 was only 5.0°, and the linkage between these two planes was conjugated with bond lengths of 1.459(6) (C19–C22), 1.302(6) (C22=C23), and 1.455(6) Å (C23–C24) (Table 2), which suggests that all non-hydrogen atoms between carbazole donor and terpyridine acceptor are highly conjugated.

Single crystals of **T2** (Fig. 2 and Table 1), suitable for the X-ray analysis, were obtained from slow evaporation of $CHCl_3$ covered with ethanol at room temperature after several days. There was disorder in crystal structure, which affects C11 and C12 in π-bridge. The disorder had two orientations, and the major part (C11A–C12A) had an occupancy factor of 0.50. As shown in Fig. 2, in the electron-acceptor moiety, the central pyridinyl (labeled P0) was also arranged with dihedral angles of 21.5° between P0 and P3, 2.2° between P0 and P4, and 2.2° between P0 and P5, indicating that the terpyridinyl is more co-planar than that in **T1**, which may be good for its electron-accepting ability. The dihedral angle between the carbazolyl plane (labeled P1) and its neighboring phenyl plane (labeled P2) was 68.2°, while the dihedral angle between planes P2 and P3 was 15.7°. The linkage between the two planes was conjugated with the bond lengths are: 1.493(5) (C10–C11), 1.338(6) (C11=C12), and 1.484(6) Å (C12–C13) (Table 2). In further survey of the π-conjugated plane, extending to the terpyridinyl group, it was revealed that the dihedral angle between P0 and P2 (5.8°) was almost the difference of that between P0 and P3 (21.5°) and that of P2 and P3 (15.7°), which shows that the π-conjugated system has become interlaced and slightly skewed.

Table 3. Photophysical Data of the Two Initiators

Compound	Solvent	λ_{max} [a]	$\lambda_{max}^{SPEF_b}$ [b]	Φ [c]	τ [d]	$\lambda_{max}^{SPEF_e}$ [e]
T1	Toluene	360	445	0.68	1.47	491
	$CHCl_3$	361	459	0.52	1.94	496
	THF	360	462	0.67	2.11	497
	Acetone	361	499	0.53	2.14	502
	DMF	364	509	0.69	2.53	516
	EtOH	362	518	0.56	2.06	521
T2	Toluene	349	430	0.93	1.53	473
	$CHCl_3$	350	446	0.87	1.91	487
	THF	348	446	0.88	2.06	490
	Acetone	347	459	0.86	2.32	497
	DMF	351	464	0.79	2.63	502
	EtOH	347	460	0.45	2.14	499

a) λ_{max} of the one-photon absorption spectra in nm. b) λ_{max} of the one-photon fluorescence spectra in nm. c) Fluorescence quantum yield. d) The lifetime of one-photon fluorescence in ns. e) λ_{max} of the two-photon fluorescence spectra in nm.

Two structural features suggest that all nonhydrogen atoms are highly conjugative, leading to eximious π-bridges for the charge transfer from carbazolyl to pyridyl. As shown in Figs. 1 and 2, it was found that the C=C exists in *trans*-isomer, which provides further evidences to support that this facile synthetic technique is efficient in constructing practical π-conjugated or π-delocalized systems of optical dye molecules.[6c,13]

Linear Absorption Spectra and Single-Photon-Excited Fluorescence (SPEF). The photophysical properties of the two compounds are summarized in Table 3. The linear absorption spectra of two compounds were measured in solvents with different polarities at a concentration of 1×10^{-5} mol L^{-1}. The SPEF spectra were measured with the same concentration as that of the linear absorption spectra. As shown in Table 3, there were visible blue-shifts from the peak positions (absorption and SPEF spectra) of **T1** to those of **T2** in the same solvent polarity. The linear absorption and SPEF spectra of the two compounds in DMF are shown in Fig. 3, as well as these visible shifts. As shown in the molecular structures, the structure modification occurs only in terminal electron-donor group. The sequence in the blue-shifts was explained by the electron-donating strength of donor groups. It is well known that a strong electron donor can stabilize the charge-separated excited state of a molecule. It indicates that **T1** contains the stronger donor. Investigating the structure of **T2**, we found that the carbazolyl plane had a big dihedral angle (68.2°) to the next phenyl plane (serious twist of the carbazolyl units to the π-bridges). Thus, the lone electron pair may be delocalized onto the carbazolyl group mainly, reducing charge transfer and molecular polarity, especially in the excited state. However, the carbazolyl plane in **T1** was coplanar with plane of the π-bridges. Thus, the carbazolyl ligand can donate more electrons than that in **T2**.

From Table 3 and Fig. 4, the maximum absorption peaks showed slight solvatochromism (less than 4 nm), the maximum fluorescence peaks clearly were red-shifted, and the fluores-

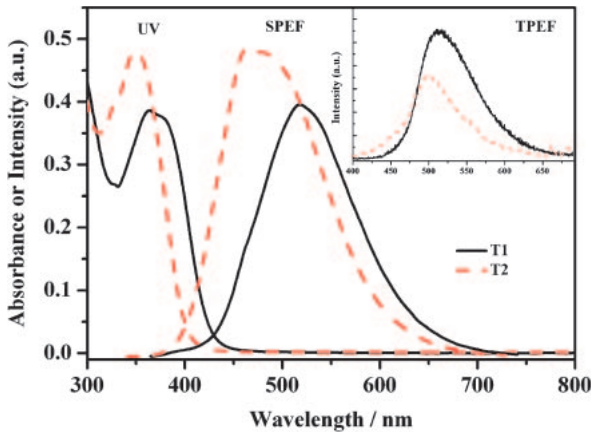

Fig. 3. Linear absorption spectra ($c = 1 \times 10^{-5}$ mol L^{-1}), SPEF spectra ($c = 1.0 \times 10^{-5}$ mol L^{-1}), and TPEF ($c = 1 \times 10^{-3}$ mol L^{-1}) spectra of two initiators in DMF.

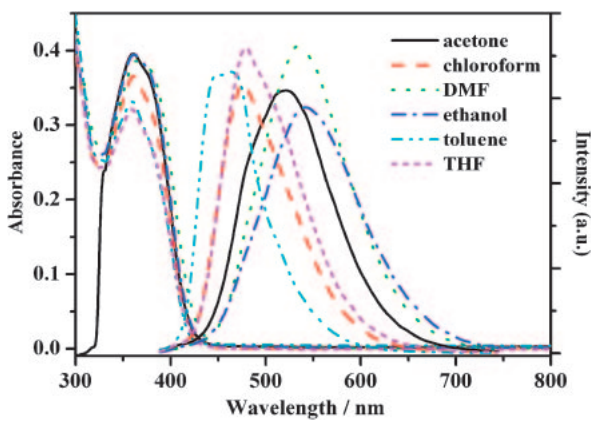

Fig. 4. Linear absorption spectra ($c = 1 \times 10^{-5}$ mol L^{-1}) and SPEF spectra ($c = 1.0 \times 10^{-5}$ mol L^{-1}) of **T1** in various solvents.

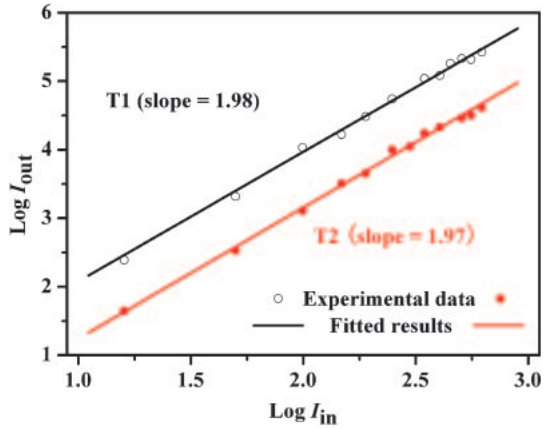

Fig. 5. The linear dependence of Log I_{out} on Log I_{in} of two initiators. Excitation carried out at 760 nm, with $c = 1.0 \times 10^{-3}$ mol L^{-1} in DMF.

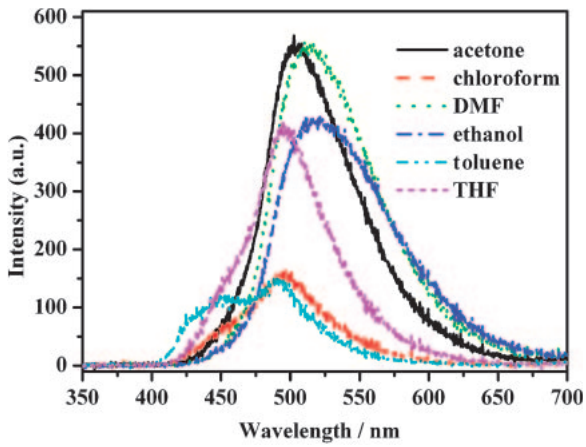

Fig. 6. TPEF spectra ($c = 1.0 \times 10^{-3}$ mol L^{-1}) of **T1** in various solvents.

cent lifetime were longer, except for ethanol, with an increase in the polarity of the solvent for each compound. This can be explained by the fact that the excited state of two compounds may possess higher polarity than that of the ground state, since solvatochromism is associated with the energy level lowering. Increased dipole–dipole interaction between the solute and solvent leads to lowering of the energy level.[16] In the case of ethanol, hydrogen bonding between the solvent and solute molecules will push the excitation energy lower.[17]

Two-Photon-Excited Fluorescence (TPEF) and Absorption (TPA). As shown in Fig. 3, there was no linear absorption in the range of 600–800 nm for two initiators, which suggests that there are no molecular energy levels corresponding to this spectral range. Therefore, upon excitation from 600 to 800 nm, it was impossible to produce single-photon-excited up-converted fluorescence. If frequency up-converted fluorescence, which is induced with a laser in this spectral range, appears, it should be mainly attributed to two-photon-excited fluorescence (TPEF). Figure 5 shows a log–log plot of the excited fluorescence signal vs excited light power. It provided direct evidence for the squared dependence of excited fluorescence power and input laser intensity.

When the concentrated solutions (1.0×10^{-3} mol L^{-1}) of the chromophores were excited by using a femtosecond laser beam with a wavelength of 720 nm, strong fluorescence with colors changing from blue to green were observed and detected (Table 3). As shown in Fig. 1 and Table 3, the TPEF spectra of two dyes were quite similar to the SPEF spectra and had similar blue-shifts from **T1** to **T2** in the same solvent. The TPEF characteristics of the compounds were also affected by their molecular environments. We found that there are similar vibronic structures and visible solvatochromism in the TPEF and SPEF spectra (Fig. 6). This implies that they come from the same fluorescent excited state. In addition, we also observed greater red-shifts in the peak positions of in the TPEF spectra relative to their corresponding SPEF with a decrease in the polarity of the solvent for each compound (Table 3). This is due to re-absorption of the fluorescence in the concentrated solution. However, when the Stokes' shifts are large enough that the emission and absorption bands hardly overlap, this re-absorption is weakened. It was concluded that the smaller the solvent polarity, the smaller the Stokes' shifts, and more visible the red-shifts from λ_{max}^{TPEF} to λ_{max}^{SPEF}.

The TPA cross-sections were measured using the two-photon-induced fluorescence technique with the following equation:[18]

$$\sigma = \sigma_{\mathrm{ref}} \frac{\Phi_{\mathrm{ref}}}{\Phi} \frac{c_{\mathrm{ref}}}{c} \frac{n_{\mathrm{ref}}}{n} \frac{F}{F_{\mathrm{ref}}}, \quad (1)$$

where ref stands for the reference molecule, σ is the TPA cross-section value, c is the concentration of solution, n is the refractive index of the solution, F is the TPEF integral intensities of the solution emitted at the exciting wavelength, and Φ is the fluorescence quantum yield. The σ_{ref} value was taken from the literature. By referencing the TPA cross-section of flouorescein to be 19 GM ($1\,\mathrm{GM} = 10^{-50}\,\mathrm{cm}^4\,\mathrm{s\,photon}^{-1}$),[19] the obtained TPA cross-sections of the two initiators were 128 and 68 GM, respectively. According to Albota et al.,[20] the terminal substitution with strong electron donors causes an increase in electron delocalization in the excited state, resulting in a substantial increase in the transition dipole moment, which is the major contributor to the enhanced TPA cross-section. The experimental results basically satisfied this principle.

Theoretical Calculation of Two-Photon Cross Sections. The transition probability of one-photon absorption (OPA) is given by an oscillator strength, where μ_α is the electric dipole moment operator, ω_f denotes the excitation

$$\delta_{\mathrm{op}} = \frac{2\omega_f}{3} \sum_{\alpha} |\langle 0|\mu_\alpha|f\rangle|^2 \quad (2)$$

energy of the excited state $|f\rangle$, $|0\rangle$ denotes the ground state, and the summation is performed over the x, y, and z axes of the molecule.

In terms of sum-over-state formula, the two-photon matrix element for the two-photon resonant absorption of identical energy[21] is written as

$$S_{\alpha\beta} = \sum_j \left[\frac{\langle 0|\mu_\alpha|j\rangle\langle j|\mu_\beta|f\rangle}{\omega_j - \omega_f/2} + \frac{\langle 0|\mu_\beta|j\rangle\langle j|\mu_\alpha|f\rangle}{\omega_j - \omega_f/2} \right], \quad (3)$$

where $|0\rangle$ and $|f\rangle$ denote the ground state and the final state, respectively, $|j\rangle$ stands for all the intermediate states, including the ground state, ω_j is the excitation energy of the excited states, and μ is the electronic dipole moment. In general, the total TPA probability requires the information for all of the excited states, which is difficult to obtain. On the other hand, a few-state model often provides reasonable results for TPA cross-section in a visible region.[20] The TPA cross-section is given by orientational averaging over the two-photon absorption probability[22]

$$\delta_{\mathrm{tpa}} = \sum_{\alpha\beta} \left[F \times S_{\alpha\alpha} S^*_{\beta\beta} + G \times S_{\alpha\beta} S^*_{\alpha\beta} + H \times S_{\alpha\beta} S^*_{\beta\alpha} \right], \quad (4)$$

where the coefficients F, G, and H are related to the incident radiation. For linearly polarized light, F, G, and H are 2, 2, and 2, but for ircular polarized light, they are -2, 3, and 3, respectively. In the present work, we only consider the results with the linearly polarized laser beam. The summation goes over the molecular axes α, $\beta = \{x, y, z\}$.

The TPA cross-section directly comparable with experimental measurements is defined as

$$\sigma_{\mathrm{tpa}} = \frac{4\pi^2 a_0^5 \alpha}{15 c_0} \frac{\omega^2 g(\omega)}{\Gamma_f} \delta_{\mathrm{tpa}}, \quad (5)$$

where a_0 is the Bohr radius, c_0 is the speed of light, α is the fine structure constant, $\hbar\omega$ is the photon energy of the incident light, $g(\omega)$ denotes the spectral line profile, which is assumed to be a δ-function., and Γ_f is the lifetime broadening of the final state, which is assumed to be 0.1 eV.[23]

We utilized the Gaussian-98 program package to optimize the molecular geometrical structure hybrid density functional theory (DFT/B3LYP) and a basis set 6-31G. The few-state model is used to study the TPA cross-section of the molecules. The calculated largest TPA cross-sections of both molecules were 2060 and 1510 GM, respectively. The calculation results were bigger than the experimental results and reasonably predicted the dependence of TPA σ value on the structure variation. Considering the sensitivity of TPA σ on measurement conditions, such as solvent, intensity level, and the pulse duration of the laser beam, we think that the calculated σ values are acceptable. Therefore, the theoretical and experimental results provide powerful evidence that these dyes can be used as sensitive two-photon polymerization initiators.

Two-Photon-Initiating Polymerization Microfabrication. In our TPIP experiments, three-dimensional cross-linked lattice periodic microstructures were fabricated with negative resins system that contained oligomer (methyl methacrylate) and 0.5% of **T1** or **T2** as initiator and a little 1,2-dichloroethane, which increased the compatibility and helped to control the viscosity. The same mode-locked Ti:sapphire laser that was used in the TPF measurements was utilized for TPMF at 720 nm. The laser was tightly focused via an objective lens (×50, NA = 0.45), and the focal point was modulated in the gel resin, which was on a *xyz*-step monitored stage, with a speed of $80\,\mu\mathrm{m\,s}^{-1}$. The pulse energy after being focused by the objective lens was ≈30 mW. Polymerization was observed with a polarization microscope (Opton, Germany), and the photographs of the microstructures were shown in Fig. 7a. The polymerization solid skeletons were uniform and orderly, and their width was about 3 μm. The distance between neighboring streaks was 10 μm. The polymerization reaction did not take place in the part out of the laser focus, which is easily washed out by tetrahydrofuran (Fig. 7b). In order to further explore the fabrication of practical devices, we designed and introduced artificial defects into the microstructures. Figure 7b shows that simple defects were introduced successfully, which is necessary for applied micro devices sometimes. The microstructures were stable for a long time in air without volume shrinkage and distortion. The polymerization reaction in the skeletons went to completion, and the inner structure was compact and rigid.

According to Cumpston et al.,[6a] strong donor substituents

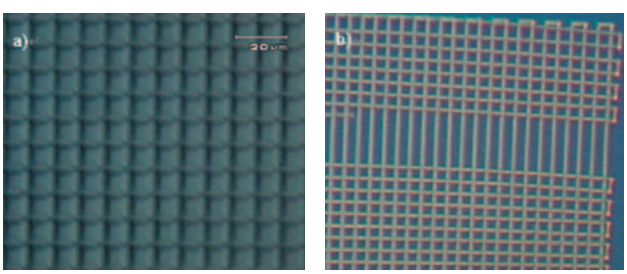

Fig. 7. Optical micrographs of the lattice fabricated via two-photon polymerization using **T1** as an initiator.

using **T1** as an initiator

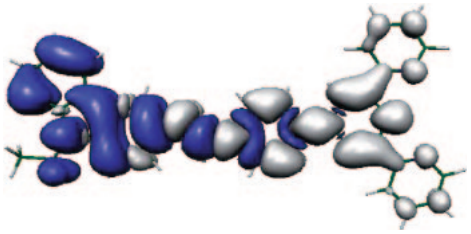

Fig. 8. Density difference between the charge-transfer and ground states of **T1** in the gas phase. Gray and blue areas represent the electron loss and gain, respectively, upon the excitation.

can make the conjugated system electron rich, and after one- or two-photon photoexcitation, the molecule is able to transfer an electron even to relatively weak acceptors, and this process can be used to activate the polymerization reaction. In order to demonstrate this process, we undertook a theoretical investigation. Our ab initio calculations using time-dependent hybrid density functional theory with the B3LYP basis set in Gaussian package for the **T1** molecule showed that the first excited state is the charge-transfer (CT) state with the excited energy $\lambda =$ 396 nm. When the molecule is irradiated by 720 nm laser beam, it can be expected that the molecule will simultaneously absorb two photons and is excited to the first excited state (the CT state). For a better understanding of the charge-transfer process, we plotted the charge density difference between the ground and the CT states for BPYPA in the gas phase (see Fig. 8), which was visualized by using MOLEKEL program.[24] From Fig. 8, it was clear that upon the excitation, charges are mainly distributed at the carbazolyl terminal of **T1**, indicating that the molecule could give away its electrons to its surroundings. This picture seems to support the Cumpston's discussion.[6a] However, whether the photoinduced electron-transfer reaction is energetically feasible needs to be further theoretically investigated.

Conclusion

In conclusion, we reported two D–π–A-type functional terpyridine derivatives which are efficient TPA initiators. The structure/properties relationships were discussed. The experimental and theoretical results revealed that the compounds with excellent SPEF and TPEF properties can be obtained by conjugating different terminals with terpyridyl groups. The photopolymerization reactions were successfully initiated by the two initiators. It was verified that the present synthetic approaches are very practical to prepare efficient two-photon initiators. It is noteworthy that facile syntheses were employed in building these terpyridine derivatives, demonstrating that it is easy to construct efficient complicated hetero-aromatic TPA initiators for realizing cheaper TPIP technology using safer and greener methods.

This work was supported by a grant for the National Natural Science Foundation of China (Nos. 50532030, 50325311, and 50335050), Doctoral Program Foundation of the Ministry of Education of China, Education Committee of Anhui Province (Nos. 2006KJ032A and 2006KJ135B), Key Foundation of the Ministry of Education of China (No. 06060347), Team for Scientific Innovation Foundation of Anhui Province (No. 2006KJ007TD) and Person with Ability Foundation of Anhui Province (No. 2002Z021). We also wish to thank Prof. D. Q. Wang of Liao Cheng University for his assistance with the X-ray structure determinations.

References

1 a) J. E. Ehrlich, X. L. Wu, L. Y. Lee, Z. Y. Hu, H. Roeckel, S. R. Marder, J. Perry, *Opt. Lett.* **1997**, *22*, 1843. b) C. W. Spangler, *J. Mater. Chem.* **1999**, *9*, 2013.

2 a) H. Stiel, K. Tenchner, A. Paul, W. Freyer, D. Leupold, *J. Photochem. Photobil., A* **1994**, *80*, 289. b) P. K. Frederiksen, M. Jorgensen, P. R. Ogilby, *J. Am. Chem. Soc.* **2001**, *123*, 1215.

3 a) G. S. He, R. Signorini, P. N. Prasad, *Appl. Opt.* **1998**, *375*, 720. b) G. S. He, L. X. Yuan, P. N. Prasad, A. Abbotto, A. Facchetti, G. A. Pagani, *Opt. Commun.* **1997**, *140*, 49.

4 a) W. Denk, J. H. Strickler, W. W. Webb, *Science* **1990**, *248*, 73. b) K. D. Belfield, K. J. Schafer, Y. Liu, J. Liu, X. Ren, E. W. Van Stryland, *J. Phys. Org. Chem.* **2000**, *13*, 837.

5 a) H. E. Pudavar, M. P. Joshi, P. N. Prasad, B. A. Reinhardt, *Appl. Phys. Lett.* **1999**, *74*, 1338. b) K. D. Belfield, K. Schafer, *Chem. Mater.* **2002**, *14*, 3656.

6 a) B. H. Cumpston, S. P. Ananthavel, S. Barlow, D. L. Dyer, J. E. Ehrlich, L. L. Erskine, A. A. Heikal, S. M. Kuebler, I. Y. S. Lee, D. M. Maughon, J. Q. Qin, H. Röckel, M. Rumi, X. L. Wu, S. R. Marder, J. W. Perry, *Nature* **1999**, *398*, 51. b) C. Martineau, R. Anémian, C. Andraud, I. Wang, M. Bouriau, P. L. Baldeck, *Chem. Phys. Lett.* **2002**, *362*, 291. c) Y. P. Tian, M. L. Zhang, X. Q. Yu, G. B. Xu, Y. Ren, J. X. Yang, J. Y. Wu, X. J. Zhang, X. T. Tao, S. Y. Zhang, M. H. Jiang, *Chem. Phys. Lett.* **2004**, *388*, 325. d) S. M. Kuebler, K. L. Braun, W. Zhou, J. K. Cammack, T. Yu, C. K. Ober, S. R. Marder, J. W. Perry, *J. Photochem. Photobiol., A* **2003**, *158*, 163.

7 a) Y. Ren, X. Q. Yu, D. J. Zhang, D. Wang, M. L. Zhang, G. B. Xu, X. Zhao, Y. P. Tian, Z. S. Shao, M. H. Jiang, *J. Mater. Chem.* **2002**, *12*, 3431. b) Y. X. Yan, X. T. Tao, Y. H. Sun, C. K. Wang, G. B. Xu, J. X. Yang, Y. Ren, X. Zhao, Y. Z. Wu, X. Q. Yu, M. H. Jiang, *J. Mater. Chem.* **2004**, *14*, 2995. c) Y. X. Yan, X. T. Tao, Y. H. Sun, G. B. Xu, C. K. Wang, J. X. Yang, X. Zhao, M. H. Jiang, *J. Solid State Chem.* **2004**, *177*, 3007. d) D. M. Li, H. P. Zhou, J. Q. Pu, X. J. Feng, J. Y. Wu, Y. P. Tian, X. Q. Yu, X. T. Tao, M. H. Jiang, *Chin. J. Chem.* **2005**, *23*, 1483. e) Y. X. Yan, X. T. Tao, Y. H. Sun, W. T. Yu, G. B. Xu, C. K. Wang, H. P. Zhao, J. X. Yang, X. Q. Yu, X. Zhao, M. H. Jiang, *Bull. Chem. Soc. Jpn.* **2005**, *78*, 300. f) H. P. Zhou, D. M. Li, J. Z. Zhang, Y. M. Zhu, J. Y. Wu, Z. J. Hu, J. X. Yang, G. B. Xu, Y. P. Tian, Y. Xie, X. T. Tao, M. H. Jiang, L. M. Tao, Y. H. Guo, C. K. Wang, *Chem. Phys.* **2006**, *322*, 459.

8 a) H. B. Sun, V. Mizeikis, Y. Xu, S. Juodkazis, J. Y. Ye, S. Matsuo, H. Misawa, *Appl. Phys. Lett.* **2001**, *79*, 1. b) M. P. Joshi, H. E. Pudavar, J. Swiatkiewicz, P. N. Prasad, B. A. Reianhardt, *Appl. Phys. Lett.* **1999**, *74*, 170.

9 S. Kawata, H. B. Sun, T. Tanaka, K. Takada, *Nature* **2001**, *412*, 697.

10 a) G. Fabbrini, E. Menna, M. Maggini, A. Canazza, G. Marcolongo, M. Meneghetti, *J. Am. Chem. Soc.* **2004**, *126*, 6238. b) H. M. Kim, M. Y. Jeong, H. C. Ahn, S. J. Jeon, B. R. Cho, *J. Org. Chem.* **2004**, *69*, 5749.

11 a) M. Heller, U. S. Schubert, *Eur. J. Org. Chem.* **2003**, 947.

b) H. Q. Liu, T. C. Cheung, S. M. Peng, C. M. Che, *J. Chem. Soc., Chem. Commun.* **1995**, 1787. c) P. Bonhôte, J. E. Moser, R. Humphry-Baker, N. Vlachopoulos, S. M. Zakeeruddin, L. Walder, M. Grätzel, *J. Am. Chem. Soc.* **1999**, *121*, 1324. d) H. J. Fang, C. M. Du, S. L. Qu, Y. L. Li, Y. L. Song, H. M. Li, H. B. Liu, D. B. Zhu, *Chem. Phys. Lett.* **2002**, *364*, 290. e) I. Eryazici, C. N. Moorefield, S. Durmus, G. R. Newkome, *J. Org. Chem.* **2006**, *71*, 1009.

12 a) F. Tessore, D. Roberto, R. Ugo, M. Pizzotti, S. Quici, M. Cavazzini, S. Bruni, F. D. Angelis, *Inorg. Chem.* **2005**, *44*, 8967. b) S. Righetto, S. Rondena, D. Locatelli, D. Roberto, F. Tessore, R. Ugo, S. Quici, S. Roma, D. Korystov, V. I. Srdanov, *J. Mater. Chem.* **2006**, *16*, 1439.

13 J. X. Yang, X. T. Tao, C. X. Yuan, Y. X. Yan, L. Wang, Z. Liu, Y. Ren, M. H. Jiang, *J. Am. Chem. Soc.* **2005**, *127*, 3278.

14 G. A. Reynolds, K. H. Drexhage, *Opt. Commun.* **1975**, *13*, 222.

15 X. M. Wang, Y. F. Zhou, W. T. Yu, C. Wang, Q. Fang, M. H. Jiang, H. Lei, H. Z. Wang, *J. Mater. Chem.* **2000**, *10*, 2698.

16 a) P. Fromherz, *J. Phys. Chem.* **1995**, *99*, 7188. b) U. Narang, C. F. Zhao, J. D. Bhawalkar, F. V. Bright, P. N. Prasad, *J. Phys. Chem.* **1996**, *100*, 4521.

17 C. K. Wang, P. Macak, Y. Luo, H. Ågren, *J. Chem. Phys.* **2001**, *114*, 9813.

18 C. Xu, W. W. Webb, *J. Opt. Soc. Am. B* **1996**, *13*, 481.

19 M. A. Albota, C. Xu, W. W. Webb, *Appl. Opt.* **1998**, *37*, 7352.

20 M. Albota, D. Beijonne, J. L. Brédas, J. E. Ehrlich, J. Y. Fu, A. A. Heikal, S. E. Hess, T. Kogej, M. D. Levin, S. R. Marder, D. McCord-Maughon, J. W. Perry, H. Röckel, M. Rumi, G. Subramaniam, W. W. Webb, X.-L. Wu, C. Xu, *Science* **1998**, *281*, 1653.

21 P. Cronstrand, Y. Luo, H. Ågren, *Chem. Phys. Lett.* **2002**, *352*, 262.

22 P. R. Monson, W. M. McClain, *J. Chem. Phys.* **1970**, *53*, 29.

23 P. Cronstrand, Y. Luo, H. Ågren, *J. Chem. Phys.* **2002**, *117*, 11102.

24 MOLEKEL, references in http://www.cscs.ch/molekel/.